The Cryosphere Discuss., https://doi.org/10.5194/tc-2018-139
Manuscript under review for journal The Cryosphere
Discussion started: 20 July 2018

The Cryosphere Discussions
Open Access
EGU

Brief Communication: Updated GAMDAM Glacier Inventory over the High Mountain Asia

Akiko Sakai[1],

[1] Graduate School of Environmental Studies, Nagoya University, Nagoya, Japan

Correspondence to: Akiko Sakai (shakai@nagoya-u.jp)

The Cryosphere Discuss., https://doi.org/10.5194/tc-2018-139
Manuscript under review for journal The Cryosphere
Discussion started: 20 July 2018

Abstract. The first version of the Glacier Area Mapping for Discharge from the Asian Mountains (GAMDAM) glacier inventory was the first methodologically consistent glacier inventory covering High Mountain Asia, and it underestimated glacier area because it did not include steep slopes covered with ice or snow and shadowed areas. During the process of revising the GAMDAM glacier inventory, source Landsat images were carefully selected to find images free of shadows, cloud cover, and seasonal snow cover taken from 1990 to 2010. Then, more than 90% of the glacier area in the final version of the GAMDAM glacier inventory was delineated based on summer Landsat images. The total glacier area was 100,693±15,103 km^2 and included 134,770 glaciers using 453 Landsat image scenes.

1 Introduction

Glaciers in High Mountain Asia (HMA) play a significant role in providing water resources for millions of people downstream (Bolch et al., 2012; Immerzeel et al., 2010). In addition, shrinking glaciers have led to sea level rises in the past and are expected to in the future (Marzeion et al., 2018; Huss and Hock., 2015; Radić and Hock, 2013).

Recent analysis of the elevational change in glaciers has showed that glaciers in HMA have contrasting fluctuations (Brun et al., 2017; Kääb et al., 2012, 2015; Gardner et al., 2013). Glaciers in the Himalaya and Hengduan-Shan are rapidly shrinking; however, glaciers in the Karakoram and West Kunlun are relatively stable. Analysis of the climate in glacier areas has showed that the Karakoram and West Kunlun regions are relatively stable under a global warming condition, as they are not sensitive to temperature change (Sakai and Fujita, 2017). This analysis, not only on glacier volume changes, but also on climate conditions in the glacier area, is based on a large-scale glacier inventory. Thus, it is crucial to produce an accurate glacier inventory covering the whole of HMA of homogeneous quality to show a more rigorous relation between glacier fluctuation and climate change.

Randolph Glacier Inventory(RGI) (Arendt et al., 2015; RGI Consortium, 2017) was the first glacier inventory established for global glaciers, although it have various varying quality even within the HMA. Thus far, Guo et al. (2015) have published the second Chinese glacier inventory (hereafter, "CGI2") produced by manual delineation. Mölg et al. (2018) have produced a glacier inventory of the Karakoram and Pamir region (hereafter "NM18") via automated digital glacier mapping and manual correction based on the coherence of synthetic aperture radar (SAR) images for debris-covered glaciers (Frey et al., 2012). Furthermore, they also separately delineated all debris-covered areas.

The Glacier Area Mapping for Discharge from the Asian Mountains (GAMDAM) project was carried out from February 2011 to March 2014. Its purpose was to create a glacier inventory covering HMA, between 67.4 and 103.9°E longitude and 27.0 and 54.9°N latitude. The first version of the GAMDAM Glacier Inventory (GGI) published in 2015 did not include steep slopes covered with ice or snow. Furthermore, the HMA region includes monsoon region, therefore, winter images were selected to avoid seasonal snow cover, and the shadowed parts of glacier area were dismissed. I revised the glacier inventory again selecting satellite images though from the summer (May–Sep) and I included snow-covered steep slopes and shadowed glacier area. This paper affirms the revision is complete and provides some information on the final version of the

GAMDAM glacier inventory. The abbreviated term "GGI15" refers to the first version of the GGI published by Nuimura et al. (2015) and "GGI18" to the final version (this study).

2 Data

We used 453 Landsat 5 Thematic Mapper ™ and Landsat 7 Enhanced Thematic Mapper (ETM+) Level 1T scenes for 196 path-row sets, which are available from the U.S. Geological Survey EarthExplorer (http://earthexplorer.usgs.gov/). Landsat ID and acquired date were used to delineate the glacier outlines are summarised in Table S1. It was difficult to obtain seasonal cloud-free, seasonal-snow-free, shadow-free (during summer and at a high solar angle) images during the initial setting period from 1999 to 2003 (Nuimura et al., 2015). I expanded the search period from 1990 to 2010 for the revised version and set the search month from May to September (the high-solar-angle season). In the case that part of a glacier area was covered by a cloud or snow, I searched other Landsat images focusing on the this part until finding an image in which this part is clear, as was possible. Thus, I had multiple images for one path-row scene in the same manner as that of the GGI15. I used at most nine images for one path-row scene (Figure 1).

As for a digital elevation model, ASTER-GDEM2 was used to analyse the aspect of the glaciers at each 90 m × 90 m grid.

3 Methods

3.1 Manual delineation

In this final version, all glacier outlines were manually delineated because there are abundant debris-covered glaciers in the HMA (Ojha et al., 2017; Herreid et al., 2015; Minora et al., 2016; Nagai et al., 2016) that cannot be automatically detected using a band ratio method (Paul et al., 2002). The method for delineation of glacier outlines was nearly the same as that of Nuimura et al. (2015) except for the minimum glacier sizes. Glaciers < 0.05 km^2 in area were excluded in the initial version (Nuimura et al., 2015), but in this final version the minimum glacier area was set at 0.01 km^2 because if glaciers < 0.05 km^2 in area were excluded in the GGI18, numerous small glaciers separated by dividing ridges would be missed. Furthermore, small glaciers were included as much as possible during the process of revision. Glacier outlines were delineated manually by 11 persons in the GGI15 (Nuimura et al., 2015). However, only one person conducted the revision of the GGI15 to produce the GGI18.

Nuimura et al. (2015) excluded snow or ice-covered steep slopes in the GGI15. Furthermore, they underestimated the upper headwall of glaciers that were covered with snow or ice. In the revised version, all snow- or ice-covered glacier area was included, and debris-covered areas were determined using high-resolution Google Earth images. Areas with rock glacier-like geography, e.g., flow lobes, which typically occur at the terminus of debris-covered glaciers, were omitted.

Nuimura et al. (2015) determined an uncertainty of 15% in glacier delineation using the results of five separate delineation tests. Because the revision of the GGI15 was carried out by one person, and the GGI18 is based on the GGI15, which was

delineated by several persons as previously mentioned, I assumed 15% for the uncertainty in the area as determined by Nuimura et al. (2015).

3.2 Quality of Landsat images

The GGI covers a vast region of HMA and includes both monsoon-dominant regions and regions dominated by westerly air flow (Maussion et al., 2014; Bookhagen and Burbank, 2010), thus available Landsat images considerably varied in quality. Therefore, even, though the search period was extended for the Landsat images, it was difficult to obtain clear images along several path-row scenes. I qualitatively evaluated the quality of the used Landsat images to show those path-row scenes that required correction in the future as only low quality Landsat images were available. The quality of images depends on three factors; cloud cover (Guo et al., 2015), seasonal snow cover, and shadows on the glacier area. I subjectively ranked the three factors of each used Landsat image using the three levels as follows: A: good (1), B: medium (0.5), C: poor (0) (the parenthetical value indicate score of each level). Specifically, these rankings indicate that for those ranked A there was no snow/cloud/shadow, for B there was only a moderate amount of snow/cloud/shadow, and for C there was considerable snow/cloud/shadow hampering delineation of the glacier outlines. Furthermore, a total ranking of each Landsat image (Table S1) was calculate using the average value of the three factors as follows: ≥ 0.7: A, ≥ 0.4 and < 0.7: B, > 0.4: C. Then, the quality of each path-row scene was also evaluated and ranked by average value of each image's score (≥ 0.7: A, ≥ 0.4 and < 0.7: B, > 0.4: C).

4 Results and discussion

A total of 134,770 glaciers in the GGI18 covered 100,693±15,103 km^2 in area (Table S2). The aggregated polygon files were separated into four regions: Central Asia, South Asia East, South Asia West, and North Asia limited at Sayan and Altai following the region polygon of RGI6.0 (Arendt et al., 2015; RGI Consortium, 2017). The total area of each region is summarised in Table 1, and compared to the glacier area for each region of RGI6.0. RGI6.0 included part of the GGI15 (RGI Consortium, 2017). The glacier area of the GGI18 for each region except South Asia West was greater than that of RGI6.0.

4.1 Comparison to the GGI15

I replaced glacier outlines delineated based on winter images in the GGI15 by those based on summer images in the GGI18. The glacier area ratio delineated based on summer images increased from 69% in the GGI15 to 95% in the GGI18 (Table 1). An example of a glacier outline of the GGI18 and the GGI15 were compared as shown in Fig. 2. Glacier outlines were delineated based on lower solar angle, shadow-dominated images in the GGI15, but shadowed glacier areas were added in the GGI18 based on images with a high solar angle(Fig. S1). Glacier area on north-facing slopes was included in the glacier area of the GGI18 (Fig. S2). However, the acquired year used to delineate the glacier outlines varied widely. The glacier area ratio delineated based on images acquired from 1999 to 2001 decreased from 73% (GGI15) to 48% (GGI18) (Table 1). The

distribution of glacier area for different acquired dates (month/year) in the GGI18 and GGI15 are summarised in Figs. S3 and S4. Glaciers in a monsoon-dominated region were delineated based on the non-summer (Jan.–May, Oct. Dec.) images in the GGI15 (Fig. S3a, b). Meanwhile, nearly all of the glacier area (> 90%: Table 1) was extracted based on summer (Jun. – Sep.) Landsat images (Fig. S3c).

The glacier area between 5000 and 6000 m a.s.l. of the GGI18 increased as compared to that of the GGI15 when reviewing the area-elevation distributions (Fig. S5a). The glacier area of the GGI18 increased in all area classed (Fig. S5c), although the number of glaciers increased mainly for small sized glaciers < 0.0625 km^2 (Fig. S5b). GGI18 have larger area at almost regions except Tibetan plateau comparing to GGI15 (Fig. S5d). Glaciers at the Tibetan plateau locate relatively flat terrain, then they have less effect of high relief mountain shadow.

And I also follow the rule of 'one glacier has one terminus'. But, it is difficult to figure out 'terminus' in the actual glacier, in particular, ice flow from glacier side. Then, the ice separation rule tend to be ambiguous in manual delineation. Thus, the number of glaciers depend on the size threshold and the separation method of glaciers.

4.2 Comparison to the other glacier inventories CGI2 and NM18

I compared the GGI18 to other glacier inventories; the second Chinese Glacier inventory (CGI2) (Guo et al., 2015) and a glacier inventory covering the Karakoram and Pamir regions (NM18) (Mölg et al., 2018). First, I extracted two parts of the GGI18, limited to the domains of CGI2 and NM18. Then each distribution of the glacier area-elevations showed that the glacier area of the GGI18 was less than that of CGI2 at elevations from 4000 to 5500 m a.s.l. (Fig. S6a). The glacier area of the GGI18 was less than that of NM18 at elevations from 4500 to 6000 m a.s.l. (Fig. S7a). As for the number and each glacier area, for each area class as shown in Figs. 7b, c and 8b, c the GGI18 had a large number of glaciers of smaller size (Fig. S6b and S7b), and the glaciers with a larger area size the GGI18 had a smaller area in total. This is because glaciers tended to be divided into multiple glaciers in the GGI18, while these same glaciers tended to be undivided in the NM18 and CGI2. Regional comparison between CGI2 and GGI18 (Fig. S6d) shows that glacier area are almost consistent except Henduang Shan, where the CGI2 could not update first Chinese glacier inventory. Those between NM18 and GGI18 (Fig. S7d) indicate NM18 has slightly larger area than that of GGI18 at almost regions. Because NM18 could include small glaciers, although GGI18 tend to miss such small glaciers.

The consistency of the GGI18 and the other two glacier inventories were also evaluated using an overlapping ratio. The overlapping ratios between the GGI18 limited to the NM18/CGI2 domains and the NM18/CGI2 to the total NM18/CGI2 were 87% and 86%, respectively (Table S3, S4). These values indicate each glacier polygon overlapped very well.

4.3 Glacier outlines required to revise by other satellite images

Cloud cover, seasonal snow cover, and shadows in the Landsat images hamper detection of glacier outlines. I evaluated the quality of the source Landsat images in terms of these three factors (Table S1). Fig. S8 shows the subjectively evaluated qualities of the Landsat images averaged for each path-row scene. Nearly all the path-row scenes of the Tibetan Plateau were of good quality (A). A total of 16 path-row scenes were rated "C," occurring mainly in the Hengduan Shan and not only in a monsoon-dominant region, but also in the Pamir ranges. The path-row scenes ranked "C" required revision, because they had only low-quality Landsat images. When we can obtain clear satellite images from other (or future) satellite image sources or in the future using the same source, these glacier outlines need to be revised. Sentinel-2 imagery may be suitable to revise those low quality glacier outlines, since Sentinel-2 has high resolution and its acquisition interval is shorter than Landsat.

5. Summary

The final version of the GAMDAM glacier inventory (GGI18) covers the whole of HMA and found 134,770 glaciers cover 100,693±15,103 km^2 in area. Nearly 95% of the total glacier area was delineated based on summer images. However, variability in the acquisition year of the source images was diverse. The total area increased approximately 15% compared to that of the GGI15 mainly including north-facing slopes. The quality of the source Landsat images was also subjectively evaluated. Some path-row scenes require correction in the future because of low-quality source images.

Data availability.

(Data submitted to PANGEA are under review. Those title and abstract can be revised after the review. And they are protected by password at present.)

1.Sakai, A (2018): GAMDAM glacier inventory for High Mountain Asia: Area-altitude distribution for Central Asia. https://doi.pangaea.de/10.1594/PANGAEA.891415

2. Sakai, A (2018): GAMDAM glacier inventory for High Mountain Asia: Area-altitude distribution for North Asia. https://doi.pangaea.de/10.1594/PANGAEA.891416

3. Sakai, A (2018): GAMDAM glacier inventory for High Mountain Asia: Area-altitude distribution for South Asia East. https://doi.pangaea.de/10.1594/PANGAEA.891417

4. Sakai, A (2018): GAMDAM glacier inventory for High Mountain Asia: Area-altitude distribution for South Asia West. https://doi.pangaea.de/10.1594/PANGAEA.891418

5. Sakai, A (2018): GAMDAM glacier inventory for High Mountain Asia: Central Asia in ArcGIS (shapefile) format. https://doi.pangaea.de/10.1594/PANGAEA.891419

6. Sakai, A (2018): GAMDAM glacier inventory for High Mountain Asia: North Asia in ArcGIS (shapefile) format. https://doi.pangaea.de/10.1594/PANGAEA.891420

7. Sakai, A (2018): GAMDAM glacier inventory for High Mountain Asia: South Asia East in ArcGIS (shapefile) format. https://doi.pangaea.de/10.1594/PANGAEA.891421

8. Sakai, A (2018): GAMDAM glacier inventory for High Mountain Asia: South Asia West in ArcGIS (shapefile) format. https://doi.pangaea.de/10.1594/PANGAEA.891422

Competing interests. The author declare that she has no conflict of interest.

Acknowledgements. This project was supported by a grant from the Funding Program for Next Generation World-Leading Researchers (NEXT Program, GR052) and Grants-in-Aid for Scientific Research (26257202) of the Japan Society for the Promotion of Science. I wish to thank all members of the GAMDAM project for their valuable support to produce the first version of GAMDAM Glacier Inventory.

References

Arendt, A., Bliss, A., Bolch, T., Cogley, J. G., Gardner, A. S., Hagen, J.-O., Hock, R., Huss, M., Kaser, G., Kienholz, C., Pfeffer, W. T., Moholdt, G., Paul, F., Radić, V., Andreassen, L. M., Bajracharya, S., Barrand, N. E., Beedle, M., Berthier, E., Bhambri, R., Brown, I., Burgess, E. W., Burgess, D., Cawkwell, F., Chinn, T., Copland, L., Davies, B., Angelis, H. de, Dolgova, E., Earl, L., Filbert, K., Forester, R., Fountain, A. G., Frey, H., Giffen, B., Glasser, N. F., Guo, W., Gurney, S. D., Hagg, W., Hall, D., Haritashya, U. K., Hartmann, G., Helm, C., Herreid, S., Howat, I., Kapustin, G., Khromova, T. E., König, M., Kohler, J., Kriegel, D., Kutuzov, S., Lavrentiev, I., Le Bris, R., Liu, S., Lund, J., Manley, W., Marti, R., Mayer, C., Miles, E. S., Li, X., Menounos, B., Mercer, A., Mölg, N., Mool, P., Nosenko, G., Negrete, A., Nuimura, T., Nuth, C., Pettersson, R., Racoviteanu, A., Ranzi, R., Rastner, P., Rau, F., Raup, B., Rich, J., Rott, H., Sakai, A., Schneider, C., Seliverstov, Y., Sharp, M. J., Sigurðsson, O., Stokes, C. R., Way, R. G., Wheate, R., Winsvold, S., Wolken, G., Wyatt, F., and Zheltihyna, N.: Randolph Glacier Inventory – A Dataset of Global Glacier Outlines: Version 5.0: GLIMS Technical Report, Global Land Ice Measurement from Space, 2015.

Bolch, T., Kulkarni, A., Kaab, A., Huggel, C., Paul, F., Cogley, J. G., Frey, H., Kargel, J. S., Fujita, K., Scheel, M., Bajracharya, S., and Stoffel, M.: The state and fate of Himalayan glaciers, Science (New York, N.Y.), 336, 310–314, doi:10.1126/science.1215828, 2012.

Bookhagen, B. and Burbank, D.: Toward a complete Himalayan hydrological budget: spatiotemporal distribution of snowmelt and rainfall and their impact on river discharge, Journal of Geophysical Research, 115, F03019, doi:10.1029/2009JF001426, 2010.

Brun, F., Berthier, E., Wagnon, P., Kääb, A., and Treichler, D.: A spatially resolved estimate of High Mountain Asia glacier mass balances, 2000-2016, Nature Geoscience, 10, 668–673, doi:10.1038/NGEO2999, 2017.

Frey, H., Paul, F., and Strozzi, T.: Compilation of a glacier inventory for the western Himalayas from satellite data: Methods, challenges, and results, Remote Sensing of Environment, 124, 832–843, doi:10.1016/j.rse.2012.06.020, 2012.

Gardner, A. S., Moholdt, G., Cogley, J. G., Wouters, B., Arendt, A. A., Wahr, J., Berthier, E., Hock, R., Pfeffer, W. T., Kaser, G., Ligtenberg, S. R. M., Bolch, T., Sharp, M. J., Hagen, J. O., van den Broeke, M. R., and Paul, F.: A reconciled estimate of glacier contributions to sea level rise: 2003 to 2009, Science, 340, 852–857, doi:10.1126/science.1234532, 2013.

Guo, W., Liu, S., Xu, J., Wu, L., Shangguan, D., Yao, X., Wei, J., Bao, W., Yu, P., Liu, Q., and Jiang, Z.: The second Chinese glacier inventory: Data, methods and results, Journal of Glaciology, 61, 357–372, doi:10.3189/2015JoG14J209, 2015.

Herreid, S., Pellicciotti, F., Ayala, A., Chesnokova, A., Kienholz, C., Shea, J., and Shrestha, A.: Satellite observations show no net change in the percentage of supraglacial debris-covered area in northern Pakistan from 1977 to 2014, Journal of Glaciology, 61, 524–536, doi:10.3189/2015JoG14J227, 2015.

Huss, M., Hock, R.: A new model for global glacier change and sea-level rise. Frontiers in Earth Science 3:54. doi: 10.3389/feart.2015.00054, 2015.

Immerzeel, W. W., van Beek, L. P. H., and Bierkens, M. F. P.: Climate change will affect the Asian water towers, Science (New York, N.Y.), 328, 1382–1385, doi:10.1126/science.1183188, 2010.

Kääb, A., Berthier, E., Nuth, C., Gardelle, J., and Arnaud, Y.: Contrasting patterns of early twenty-first century glacier mass change in the Himalayas, Nature, 488, 495–498, doi:10.1038/nature11324, 2012.

Kääb, A., Treichler, D., Nuth, C., and Berthier, E.: Brief Communication: Contending estimates of 2003-2008 glacier mass balance over the Pamir-Karakoram-Himalaya, The Cryosphere, 9, 557–564, doi:10.5194/tc-9-557-2015, 2015.

Marzeion, B., Kaser, G., Maussion, F., Champollion, N.: Limited influence of climate change mitigation on short-term glacier mass loss. Nature Climate Change, 8, 305–308, doi:org/10.1038/s41558-018-0093-1, 2018.

Maussion, F., Scherer, D. Mölg, T. Collier, E. Curio, J., and Finkelnburg, R.: Precipitation seasonality and variability over the Tibetan Plateau as resolved by the High Asia Reanalysis, Journal of Climate, 27, 1910–1927, doi:10.1175/JCLI-D-13-00282.1, 2014.

Minora, U., Bocchiola, D., D'Agata, C., Maragno, D., Mayer, C., Lambrecht, A., Vuillermoz, E., Senese, A., Compostella, C., Smiraglia, C., and Diolaiuti, G. A.: Glacier area stability in the Central Karakoram National Park (Pakistan) in 2001–2010, Progress in Physical Geography, 40, 629–660, doi:10.1177/0309133316643926, 2016.

Mölg, N., Bolch, T., Rastner, P., Strozzi, T., and Paul, F.: A consistent glacier inventory for the Karakoram and Pamir regions derived from Landsat data: distribution of debris cover and mapping challenges, Earth System Science Data Discussions, https://doi.org/10.5194/essd-2018-35, in review, 2018.

Nagai, H., Fujita, K., Sakai, A., Nuimura, T., and Tadono, T.: Comparison of multiple glacier inventories with a new inventory derived from high-resolution ALOS imagery in the Bhutan Himalaya, The Cryosphere, 10, 65-85, https://doi.org/10.5194/tc-10-65-2016, 2016.

Nuimura, T., Sakai, A., Taniguchi, K., Nagai, H., Lamsal, D., Tsutaki, S., Kozawa, A., Hoshina, Y., Takenaka, S., Omiya, S., Tsunematsu, K., Tshering, P., and Fujita, K.: The GAMDAM glacier inventory: a quality-controlled inventory of Asian glaciers, The Cryosphere, 9, 849-864, https://doi.org/10.5194/tc-9-849-2015, 2015.

Ojha S, Fujita K, Sakai A, Nagai H, Lamsal D.: Topographic controls on the debris-cover extent of glaciers in the Eastern Himalayas: Regional analysis using a novel high-resolution glacier inventory. Quaternary International, 455, 82-92, doi:10.1016/j.quaint.2017.08.007, 2017.

Paul, F., Kääb, A., Maisch, M., Kellenberger, T., and Haeberli, W.: The new remote-sensing-derived Swiss glacier inventory: I. Methods, Annals of Glaciology, 34, 355–361, doi:10.3189/172756402781817941, 2002.

Radić, V., Hock, R.: Glaciers in the Earth's hydrological cycle: Assessments of glacier mass and runoff changes on global and regional scales, Surveys in Geophysics, 1–25, doi: 10.1007/s10712-013-9262-y, 2013.

RGI Consortium: Randolph Glacier Inventory 6.0, (https://www.glims.org/RGI/) 2017.

Sakai, A., Nuimura, T., Fujita, K., Takenaka, S., Nagai, H., and Lamsal, D.: Climate regime of Asian glaciers revealed by GAMDAM glacier inventory, The Cryosphere, 9, 865-880, https://doi.org/10.5194/tc-9-865-2015, 2015.

Sakai A, Fujita K: Contrasting glacier responses to recent climate change in high-mountain Asia, Scientific Reports, 7(1), 13717, doi:10.1038/s41598-017-14256-5, 2017.

The Cryosphere Discuss., https://doi.org/10.5194/tc-2018-139
Manuscript under review for journal The Cryosphere
Discussion started: 20 July 2018

Table 1. Comparison between the GGI15 and GGI18. Total glacier area and glacier area ratio based on summer images that are based on images acquired from 1999 to 2001 are listed.

	GGI15 Nuimura et al.(2015)	GGI18 This study
Minimum glacier area (km^2)	0.05	0.01
Total area (km^2)	87,583	100,693
Total number	87,084	134,770
Used Landsat images	356	453
Glacier area based on summer (JJAS) images (%)	69	95
Glacier area based on images acquired from 1999 to 2001 (%)	73	48

5

The Cryosphere Discuss., https://doi.org/10.5194/tc-2018-139
Manuscript under review for journal The Cryosphere
Discussion started: 20 July 2018

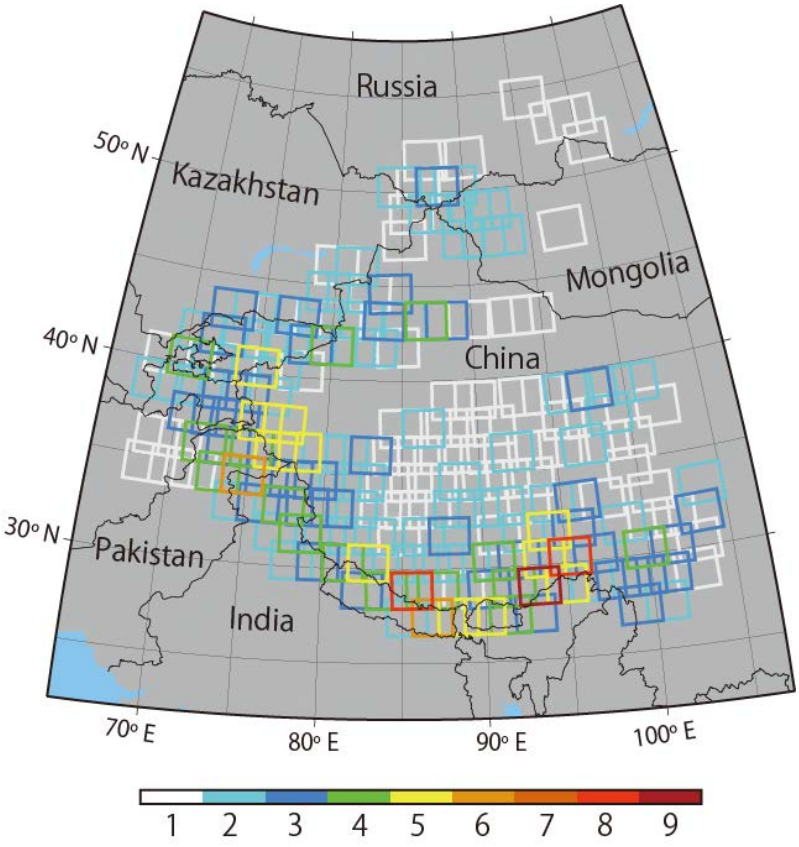

Figure 1: Footprints of the Landsat scenes used in the GGI18. The colours indicate the number of scenes used to delineate the glacier outlines.

The Cryosphere Discuss., https://doi.org/10.5194/tc-2018-139
Manuscript under review for journal The Cryosphere
Discussion started: 20 July 2018

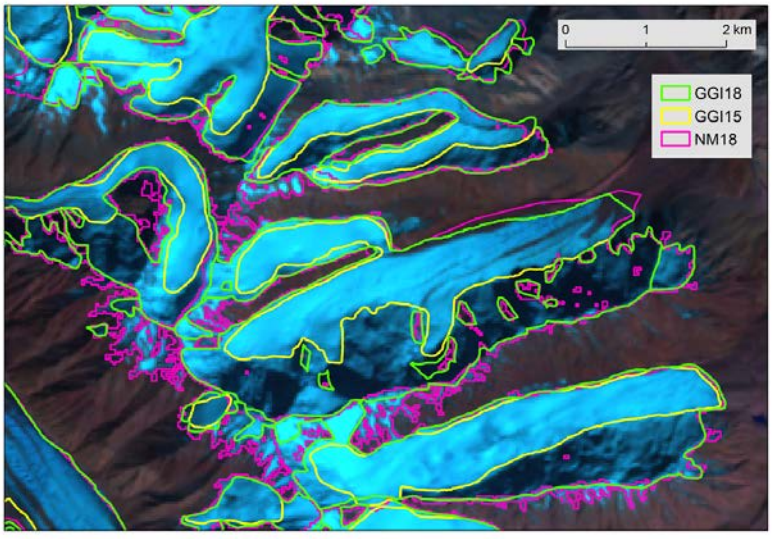

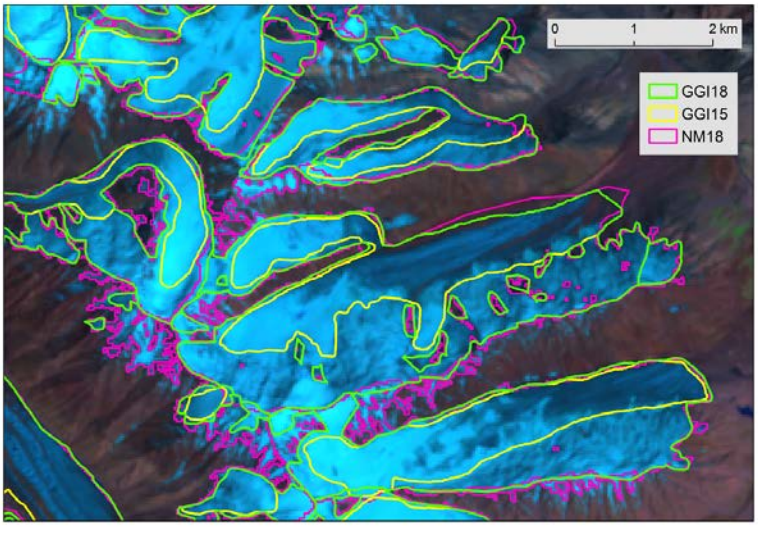

Figure 2: Comparison of the glacier outlines of each glacier inventory, GGI15, GGI18, and NM18, at 72°25'18"E, 38°55'25"N (path151 row33 of WRS2). The backgrounds are false colour (bands 7, 4, and 2 as RGB) composite Landsat images taken on 28 September 2001 (above), and 26 July 2001(below), respectively. Glacier outlines of the GGI15 (yellow line) were delineated based on the above (much shadow)image, and those of the GGI18 (green line) were delineated based on the below (less shadow) image. The glacier outlines of NM18 (Mölg et al., 2018) are also shown for comparison.